Performance Evaluation of RAKE Receiver for UWB Systems using Measured Channels in Industrial Environments

Muhammad Gufran Khan, Jörgen Nordberg, Abbas Mohammed, Ingvar Claesson
Department of Signal Processing, School of Engineering,
Blekinge Institute of Technology, SE-372 25 Ronneby, Sweden
Email: {Muhammad.Gufran.Khan, Jorgen.Nordberg, Abbas.Mohammed, Ingvar.Claesson}@bth.se

***Abstract*— The industrial environments are an important scenario for ultra wideband (UWB) communication systems. However, due to large number of metallic scatterers in the surroundings, the multipath offered by UWB channels is dense with significant energy. In this paper, the performance of RAKE receivers operating in a non line-of-sight (NLOS) scenario in these environments is evaluated. The channels used for the evaluation are measured in a medium-sized industrial environment. In addition, a standard IEEE 802.15.4a channel model is used for comparison with the results of the measured data. The performance of partial RAKE (PRake) and selective RAKE (SRake) is evaluated in terms of uncoded bit-error-rate (BER) using different number of fingers. The performance of maximal ratio combining (MRC) and equal gain combining (EGC) is compared for the RAKE receiver assuming perfect knowledge of the channel state. Finally, based on the simulation results, conclusions are drawn considering the performance and complexity issues for system design in these environments.**

I. Introduction

Ultra-wideband (UWB) radio is emerging worldwide as a particularly appealing transmission technique for applications requiring either high bit rates over short ranges or low bit rates over medium-to-long ranges [1]. The wide unlicensed frequency band assigned by US Federal Communications Commission (FCC) [2] enables a very high data rate, that is particularly suitable for wireless personal area networks (WPANs). The low data rate applications, in which impulse radio (IR) UWB is a promising physical layer candidate, include e.g., sensor networks, wireless body area networks (WBANs), localization and ranging. The IEEE 802.15.4a group, which is developing an alternative physical layer standard for low data rate systems combined with ranging capability, has recognized the fact that a considerable amount of UWB devices will be deployed in industrial buildings, factories and warehouses [3]. The application set includes e.g., sensor networks for process control, supervision of storage halls, and asset tagging and management.

The characteristics of UWB propagation channels for industrial environments differ considerably from the standard office and residential environments [3]. The reported measurement results from these environments that also form the basis for the channel model developed by IEEE 802.15.4a channel modeling subgroup are given in [4], [5]. Recently, an extensive measurement campaign has been performed by the authors in an industrial environment to further investigate the UWB propagation characteristics. From these measurements, the channel parameters have been extracted for channel modeling and system design. These results have been reported in [3].

Due to large bandwidth of UWB systems, multipath components having differential delays of the order of nanoseconds (approximately equal to the inverse of the spreading bandwidth) are resolved [6]. The RAKE receiver can be used to receive these components as it exploits the time-diversity inherent in multipth and attempts to collect the signal energy coherently from the received signal paths that fall within its span [7]. However, for the environments like a factory hall with multiple metallic reflectors, the multipath environment is dense and almost all resolvable delay bins contain significant energy [4]. In this case, RAKE receiver needs to capture a large number of (on the order of hundred) multipath components (MPCs) to collect a significant amount of the received energy [3] [5]. To meet these system design challenges, it is necessary to evaluate the system performance considering realistic channel characteristics of the environment.

The performance of coherent and non-coherent receivers for UWB systems has been evaluated previously in the literature but most of these evaluations have been performed using UWB channels for office or residential environments [8], [9], [10], [11]. Moreover, in most of the previous evaluations, simulated channels based on models employing Rayleigh or Lognormal fading statistics have been used. Thus, the objective of this paper is to investigate and analyze the performance of different RAKE receivers in terms of uncoded bit-error-rate (BER) using the measured channel responses in an industrial environment. In addition, a standard IEEE 802.15.4a channel model for NLOS industrial environments is used to compare the results with that of the measured data. The dependence of achievable BER on the types of RAKE, the number of fingers and the RAKE combining schemes is evaluated. Further, based on the simulation results, performance and complexity issues for RAKE receiver design are discussed for these scenarios.

The rest of the paper is outlined as follows. In section II, the system model of a typical UWB system is described. Section III presents the UWB channels used for the performance evaluation of the system. In section IV, the performance and different types of RAKE receiver are described. In section V, the simulation parameters have been presented. The results and analysis is discussed in section VI and finally the conclusions are presented in section VII.

II. System Model

Consider a binary antipodal modulation and time-hopping impulse radio (TH-IR) UWB system as multiple-access scheme. The transmitted signal from a user u in the system can be represented as

$$s_{TX}^{(u)}(t) = \sqrt{\frac{E_b^{(u)}}{N_f}} \sum_{j=-\infty}^{\infty} d_j^{(u)} b_{\lfloor j/N_{TH} \rfloor}^{(u)} p_{tx}(t - jT_f - c_j^{(u)} T_c), \quad (1)$$

where $p_{tx}(t)$ is the transmitted UWB pulse, $E_b^{(u)}$ is the symbol energy of the user u, T_f is the frame duration, T_c is the chip duration, N_f is the number of pulses representing one binary information symbol $b_{\lfloor j/N_{TH} \rfloor}^{(u)} \in \{1, -1\}$ transmitted by user u. The pseudorandom time-hopping (TH) sequences $\{c_j^{(u)}\}$ are assigned to each user that share the UWB media to avoid catastrophic collisions among the pulses of different users. If the number of chips in a frame is denoted as N_c, then the chip interval is chosen to satisfy $T_c \leq T_f/N_c$. This avoids pulses of different users from overlapping. The pseudorandom polarity codes $d_j^{(u)} \in \{1, -1\}$ having equal probability provide robustness against multiple access interference [12]. The polarity randomization codes also help to get a zero-mean output and shape the transmit spectrum according to FCC rules [13]. As a single user is considered, the index u is suppressed for notational simplicity in remainder of the paper.

The signal for a user is transmitted through a multipath channel with discrete-time impulse response given by

$$h(t) = \sum_{l=0}^{L-1} \alpha_l \delta(t - \tau_l), \quad (2)$$

where α_l are the channel tap weights, L is the number of multipath components and τ_l is the delay associated with lth multipath component. The details of the channel are described further in the next section. The received signal can then be expressed as

$$\begin{aligned} r_{RX}(t) &= \sqrt{\frac{E_s}{N_f}} \sum_{j=-\infty}^{\infty} \sum_{l=0}^{L-1} \alpha_l d_j b_{\lfloor j/N_{TH} \rfloor} \\ &\quad \times p_{tx}(t - jT_f - c_j T_c - \tau_l) + \sigma_n n(t) \\ &= \sqrt{\frac{E_s}{N_f}} \sum_{j=-\infty}^{\infty} d_j b_{\lfloor j/N_{TH} \rfloor} \\ &\quad \times g(t - jT_f - c_j T_c - \tau_l) + \sigma_n n(t), \quad (3) \end{aligned}$$

where $g(t) = p_{tx}(t) * h(t)$, σ_n^2 is the noise variance, $n(t)$ is a zero mean unit-variance Gaussian process and $*$ denotes the convolution operation.

III. UWB Channels

In this section, the two types of channels that have been used for the performance evaluation are discussed.

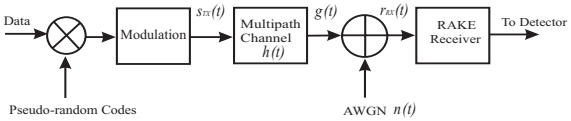

Fig. 1. Block diagram of the system model (single-user).

A. Measured UWB Channels

The measurement campaign was conducted in MAX-Lab, Lund, Sweden, a medium-sized industrial environment. The measurements were performed in the frequency domain using a vector network analyzer (VNA) in conjunction with virtual antenna arrays. The frequency range measured was from 3.1 to 8.0 GHz which resulted in a delay resolution of 0.2 ns. A total of sixteen peer-to-peer (P-P) NLOS positions were measured at four different locations with Tx-Rx separations ranging from 2 to 16 m. The use of virtual antenna arrays allows to create a virtual MIMO system of 7×7 antenna positions. Thus, for each measurement, 49 independent realizations of the channel were measured over a local area resulting in a total of 49×16 independent NLOS channel realizations. The results from these measurements were presented in the form of power delay profiles and parameters were extracted for channel modeling. A complete description of the measurement setup, the environment and analysis of the model parameters can be found in [3].

For the system evaluation, the measured channel responses are divided into two groups based on the Tx-Rx separation. The measurement group 1 (MG1) covers the distances in the range of 2 to 8 m, while the measurement group 2 (MG2) consists of the measured channel responses with Tx-Rx separation from 10 to 16 m. The total number of independent realizations for MG1 and MG2 are 490 and 294, respectively.

B. IEEE 802.15.4a Channel Model (CM8)

The IEEE 802.15.4a group has recently proposed a channel model [16] for sensor networks and similar devices with data rates between 1 kbit/s and several Mbit/s. The model which is a modified version of the original Saleh-Valenzuela (S-V) model [15] considers the arrival of multipath components in clusters as observed in many measurements e.g., [4], [3], [14]. The impulse response of the S-V model is given as in [15],

$$h(t) = \sum_{l=0}^{L-1} \sum_{k=0}^{K-1} \alpha_{k,l} \delta(t - T_l - \tau_{k,l}), \quad (4)$$

where $\alpha_{k,l}$ is the tap weight of the kth ray (path) in the lth cluster, T_l is the arrival time of the lth cluster and $\tau_{k,l}$ is the arrival time of the kth ray in the lth cluster. The key features of the IEEE 802.15.4a model include a mixed Poisson distribution for ray arrival times, possible delay dependence of cluster decay times and frequency dependence of the path loss [16]. In addition, the small scale fading statistics are modeled as Nakagami$-m$ distributed with different $m-$factors for different multipath components (MPCs). The PDF of Nakagami$-m$ distribution is given by [16],

TABLE I

COMPARISON OF CHANNEL CHARACTERISTICS

Channel characteristics	**MG1**	**MG2**	**CM8**
Distance (m)	2–8	10–16	2–8
Scenario	NLOS	NLOS	NLOS
Mean excess delay [ns]	43	62.9	113.3
RMS delay spread [ns]	51	66	87
$\text{NP}_{10[\text{dB}]}$	47.1	86.5	220.9
NP$\{85\%\}$	209.8	318.1	1137.2

$$pdf(x) = \frac{2}{\Gamma(m)}(\frac{m}{\Omega})^m x^{2m-1}\exp(-\frac{m}{\Omega}x^2), \qquad (5)$$

where $m \geq 1/2$ is the Nakagami $m-$factor, $\Gamma(m)$ is the gamma function, and Ω is the mean-square value of the amplitude i.e. mean power. The $m-$parameter is modeled as a lognormally distributed random variable, logarithm of which has a mean μ_m and a standard deviation σ_m [16].

The IEEE 802.15.4a channel model covers different office, residential and industrial scenarios. The channel model which is used in the paper is for NLOS scenarios in industrial environments, referred to as CM8. In this model, particularly for some NLOS scenarios, a first increase and then decrease in power delay profile has been proposed based on the measurement results. Additionally, the impulse response assumes regular tap spacing for ray arrival times motivated by the fact that a 'dense' arrival of MPCs with significant energy was observed. The shape of the power delay profile (PDP), as in Fig. 2, can be described (on a log-linear scale) as [16],

$$E\{|a_{k,l}^2|\} = (1-\chi\exp(-\tau_{k,l}/\gamma_{\text{rise}}))\exp(-\tau_{k,l}/\gamma_1) \times \frac{\gamma_1+\gamma_{\text{rise}}}{\gamma_1}\frac{\Omega_1}{\gamma_1+\gamma_{\text{rise}}(1-\chi)}, \qquad (6)$$

where the parameter χ describes the attenuation of the first component, the parameter γ_{rise} determines how fast the PDP increases to its local maximum, and γ_1 determines the decay at late times.

For the performance comparison with the measured channels, 100 realizations of CM8 are simulated using the channel model parameters. A comparison of some characteristics averaged over different realizations of the channels is given in Table II. $\text{NP}_{10[\text{dB}]}$ is the average number of paths within 10 [dB] of the strongest path in the channel and NP $\{85\%\}$ denotes the average number of paths that contain 85 percent of the channel energy.

IV. RAKE RECEIVER

The RAKE receiver consists of a bank of correlators or matched filters also called fingers. Each RAKE finger is matched to a particular multipath component to combine the received multipaths coherently. If the receiver uses all the L received paths, it is called all RAKE (*ARake*) [6]. However, the number of multipath components that can be utilized in a typical RAKE combiner is limited by power consumption

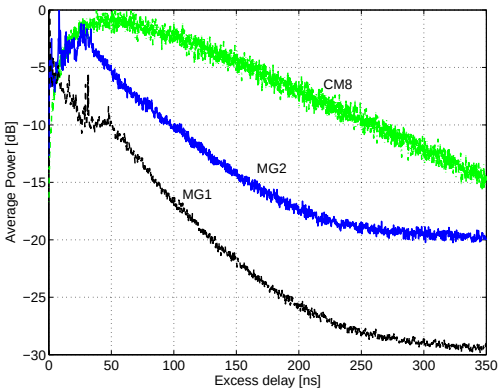

Fig. 2. Average power delay profile of MG1, MG2 and CM8 over used channel realizations.

issues, design complexity, and the channel estimation [6]. Thus, in practice, only a subset of total resolved multipath components is used, e.g., partial RAKE (*PRake*) and selective RAKE (*SRake*) use a limited number of fingers. The PRake receiver uses the M *first arriving* paths out of L resolvable multipath components, while SRake searches for the M *best paths* out of L received MPCs to use them as RAKE fingers [6].

A reference or template signal matched to the incoming received signal is used by the RAKE receiver. Each finger of the RAKE uses a delayed version of the template signal to match the delay to a specific multipath component. In order to enable *symbol-rate* sampling, the received signal is correlated with a symbol-length template signal, and the correlator output is sampled once per symbol [17]. The template signal matched to the whole pulse sequence of one information symbol is given by

$$v_{temp}(t) = \sqrt{\frac{1}{N_f}}\sum_{j=kN_f}^{(k+1)N_f-1} d_j p_{rx}(t - jT_f - c_jT_c). \qquad (7)$$

The output of the lth finger of the RAKE receiver for the kth symbol is given by

$$z_{l,k} = \int_{-\infty}^{+\infty} r_{RX}(t)v_{temp}(t-\tau_l)dt. \qquad (8)$$

Assuming a perfect match of the received signal with the reference signal, zero inter-frame and inter-symbol interference, and symbol rate sampling at the output of RAKE fingers, then (8) can be rewritten in discrete time as

$$z_{l,k} = b_k\sqrt{E_b}\alpha_l + n_{l,k}, \qquad (9)$$

where $l = 0, 1, \cdots, L-1$ and k represents the symbol index and $n_{l,k} = \sigma_n\int_{-\infty}^{+\infty} n(t)v_{temp}(t-\tau_l)dt$ is the noise at the output of the correlator which is approximately distributed as $n \sim \mathcal{N}(0, \sigma_n^2)$. The outputs of the correlators for the kth symbol can be written in vector notation as

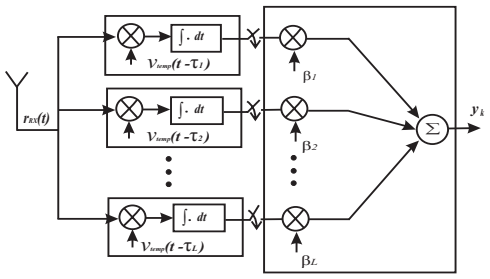

Fig. 3. A RAKE receiver structure for TH-IR UWB system.

$$\mathbf{z}_k = b_k\sqrt{E_b}\boldsymbol{\alpha} + \mathbf{n}_k, \tag{10}$$

where $\mathbf{z}_k = [z_{0,k}, \cdots, z_{L-1,k}]^T$, $\boldsymbol{\alpha} = [\alpha_0. \cdots, \alpha_{L-1}]^T$, and $\mathbf{n}_k = [n_{0,k}, \cdots, n_{L-1,k}]^T$.

Further, RAKE receivers can use different combing schemes. Let $\boldsymbol{\beta} = [\beta_0, \beta_1, \cdots, \beta_{L-1}]$ be the RAKE combining weights. If maximal ratio combining (MRC) technique is used, the amplitudes of the received MPCs are estimated and are used as wieghing vector $\boldsymbol{\beta}$ in each finger. In case of ARake, the combining weights are chosen as $\boldsymbol{\beta} = \boldsymbol{\alpha}$, where $\boldsymbol{\alpha} = [\alpha_0, \alpha_1, \cdots, \alpha_{L-1}]$ are the fading coefficients of the channel. If the set of indices of the M best fading coefficients with largest amplitude is denoted by $\mathcal{S}$, then the combining weights $\boldsymbol{\beta}$ of an SRake are chosen as follows [18],

$$\boldsymbol{\beta} = \begin{cases} \alpha_l, & l \in \mathcal{S} \\ 0, & l \notin \mathcal{S} \end{cases}. \tag{11}$$

Similarly, for PRake using the first M multipath components, the weights of MRC combining are given by [18],

$$\boldsymbol{\beta} = \begin{cases} \alpha_l, & l = 0, \cdots, M-1 \\ 0, & l = M, \cdots, L-1 \end{cases} \tag{12}$$

where $M \leq L$. In case of equal gain combining (EGC) scheme, all the tracked MPCs are weighted with their corresponding signs and combined [8]. The output after RAKE combining is sent to the decision device and can be written as

$$y_k = b_k\sqrt{E_b}\sum_{l=0}^{L-1}\beta_l\alpha_l + n_k. \tag{13}$$

To determine the bit error probability (BEP) at the output of the RAKE, the output signal-to-noise (SNR_o) needs to be evaluated. From (13), the approximate signal energy and the noise variance at the output of RAKE are evaluated as

$$E(signal^2) = E_b(\sum_{l=0}^{L-1}\beta_l\alpha_l)^2, \tag{14}$$

$$E(noise^2) = \sigma_n^2\sum_{l=0}^{L-1}{\beta_l}^2. \tag{15}$$

In case of binary antipodal modulation, for a given SNR per bit γ_b, the approximate expression of BEP conditioned on a particular channel realization is given by [7],

$$\begin{aligned} P_{e|\boldsymbol{\alpha}}(\gamma_b) &= Q(\sqrt{SNR_o}) \\ &\approx Q\left(\frac{\sqrt{E_b(\sum_{l=0}^{L-1}\beta_l\alpha_l)^2}}{\sqrt{\sigma_n^2\sum_{l=0}^{L-1}{\beta_l}^2}}\right), \end{aligned} \tag{16}$$

here $Q(\cdot)$ is the standard Q function [7].

However, to obtain the error probabilities when channel fading coefficients $\boldsymbol{\alpha}$ are random e.g., Nakagami$-m$ fading coefficients in our case, we must average the $P_e(\gamma_b)$ over the probability density function of γ_b [7], as

$$P_e = \int_0^\infty P_e(\gamma_b)p(\gamma_b)d\gamma_b. \tag{17}$$

By evaluating the probability distribution function of output SNR, average BEP can be obtained. It is difficult to obtain a closed-form expression of (17), however, this average can be evaluated numerically, or by employing Monte-Carlo simulations.

V. Simulation Parameters

In order to compare the performance of RAKE receivers on the NLOS multipath channels described in section III, the UWB system is simulated for an indoor industrial environment. The simulation parameters are as follows:

- The binary antipodal modulation is used employing second derivative of the Gaussian pulse.
- The pulse duration is kept 1.02 ns and 0.625 ns over measured and simulated channels, respectively.
- The uncoded data rate of 4 Mbps is achieved with $N_f = 10$ and $T_f = 25$ ns.
- A frame time of $T_f = 25$ ns results in inter-frame interference (IFI) as it is less than the delay spread introduced by the channels.
- The energy of the channel impulse response is normalized as $\sum\alpha_l^2 = 1$.
- The system is assumed to be synchronized with perfect knowledge of the channel characteristics.

The performance over the channels is evaluated using 490, 294 and 100 channel realizations of MG1, MG2 and CM8 respectively, for each E_b/N_o. The simulations are performed until 200 bit errors has been detected or at least $100,000$ bits has been transmitted.

VI. Simulation Results

In this section, the simulation results are analyzed. In Fig. 4, the analytical expression of (14) and (15) are averaged for each channel over corresponding number of realizations. The output SNR (SNR_o) is shown versus the number of MPCs captured by PRake and SRake over MG1, MG2 and CM8. The results demonstrate an increase in SNR_o with the increase in number of fingers. It is observed that the increase in SNR with the increase in number of captured MPCs is low for PRake as

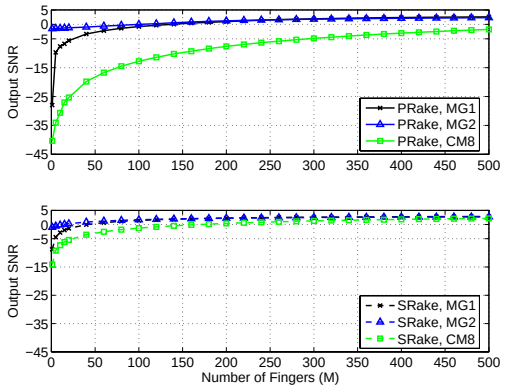

Fig. 4. Output SNR vs Number of RAKE fingers on MG1, MG2 and CM8 PRake (top) and SRake(bottom).

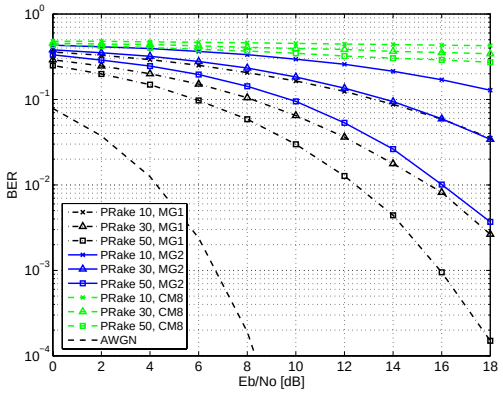

Fig. 5. Comparison of BER of different number of fingers of PRake with MRC combining on MG1, MG2 and CM8.

compared to SRake. Moreover, the dependence of SNR_o over the channel models is also observed. The gain in SNR_o as the number of fingers increases is much higher in case of MG1 up to a certain number of fingers. It is noteworthy that this is particularly depicted by PRake receiver. It is also observed that the SNR improvement is significant by increasing the number of fingers up to 100 for PRake and 50 for SRake. However, the saturation effects are observed by any further increase as the rest of the components do not carry significant energy. It can be concluded that any further increase in the number of fingers increases the complexity of the system and does not provide much SNR gain. This is particularly true for the channels having a shape of the PDP similar to MG1 and MG2.

Fig. 5 presents the results of PRake receiver with MRC combining using different number of fingers. The results are shown for both measured and simulated channels. The results demonstrate that the performance of PRake receiver largely depends on the shape of channel profile. As PRake captures only the first arriving components, the performance severely degrades on CM8 as compared to MG1 and MG2. This is quite intuitive as CM8 has first increasing and then decreasing power delay profile. The power delay profile of MG2 also has a shape of first increasing and then decreasing PDP, see Fig. 2. However, in contrast to CM8, the PDP of MG2 has a fast increase to its local maximum and also the decay is fast at late times. In addition, there are some strong components in the PDP indicating the arrival of MPCs in clusters. On the other hand, MG1 has a decreasing PDP with embedded strong components at shorter delays indicating the onset of clusters of MPCs.

It is shown in Fig. 5 that the BER is very high even with 50 PRake fingers particularly over CM8. To further improve the BER, PRake need to use on the order of hundred fingers that increases the complexity of the receiver significantly. In the case of MG2, it is possible to achieve a BER of 10^{-2} using $M = 50$ fingers with $E_b/N_o = 16$ dB. However, the results show that by using 30 fingers of the PRake receiver, it is not possible to achieve a BER of 10^{-2} even with $E_b/N_o = 18$ dB.

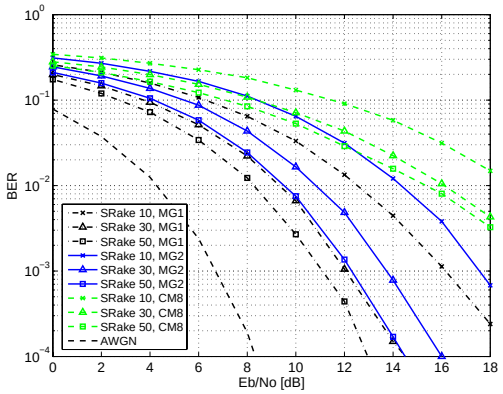

Fig. 6. Comparison of BER of different number of fingers of SRake with MRC combining on MG1, MG2 and CM8.

In Fig. 6, the performance of SRake receiver has been analyzed using different number of fingers with MRC combining over the UWB channels. The results demonstrate a significant performance improvement using SRake as compared to PRake. The results for CM8 indicate that it is possible to achieve a BER of 10^{-2} with $E_b/N_o = 16$ dB using 30 fingers of the SRake. The results over MG2 show that 30 SRake fingers can provide a BER of 10^{-3} with $E_b/N_o = 13.5$ dB . It is also observed that the same BER can be achieved using only 10 fingers of SRake over MG2 with $E_b/N_o = 17.5$ dB. Moreover, the performance of SRake is also better over MG1 than over MG2 and CM8. For MG1, the results of Fig. 6 demonstrate that a BER of 10^{-3} is achieved with only 10 fingers of the SRake with E_b/N_o of about 16 dB. Moreover, a 4 dB SNR gain is achieved for the same BER of about 10^{-3} if 30 fingers of the SRake receiver are used.

When compared with PRake receiver, it is observed that SRake can achieve much better performance. This is particularly true for the channels having a shape of the PDP similar to CM8. In case of MG2, the SRake performance using only 10 fingers is better than using 50 fingers of PRake. While

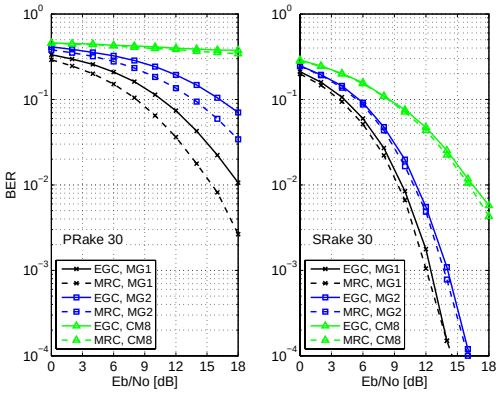

Fig. 7. Comparison of EGC and MRC combining using 30 fingers of PRake (left) and SRake (right) on MG1, MG2 and CM8.

for MG1, the results demonstrate that 10 fingers of SRake has almost the same BER as the 50 fingers of the PRake. These results depict a significant performance improvement associated with the SRake that uses only few fingers. However, it should be mentioned that the complexity of the SRake stems from the fact that it needs to search for the 10 fingers that carry the maximum energy.

The effect of RAKE combining scheme is analyzed in Fig. 7. The BER is compared using 30 fingers of both types of RAKE using EGC and MRC combining schemes. The results show that the performance of MRC combining is better than EGC. It should be noted that over measured channels, there is some performance improvement using MRC rather than EGC combining with PRake. In contrast, the BER using EGC and MRC is almost comparable in case of SRak. In this case, the complexity of the SRake can be reduced using EGC without a significant performance degradation.

VII. Conclusions

In this paper, we have presented the performance evaluation of different types of RAKE receiver over measured and a standard IEEE 802.15.4a UWB channel for industrial environments. The simulation results show that over the measured channels with Tx-Rx separation of 2–8 m, a BER of 10^{-3} can be achieved using 30 fingers (correlators) of PRake with $E_b/N_o = 12$ dB. The SRake can give the same BER with only 10 fingers with a further SNR increase of 4 dB. For the channels measured with Tx-Rx separation of 10–16 m, PRake receiver is unable to achieve a BER of 10^{-3} even with 50 fingers and E_b/N_o of 18 dB. However, only 10 fingers of the SRake are required to achieve the same BER using E_b/N_o of 17.5 dB. The results show that the SRake receiver always outperforms the PRake using the same number of fingers and the same combining scheme. We also show that the difference in the performance of MRC and EGC combining schemes is not that significant for SRake, while PRake has a considerably better performance using MRC. The comparison of the results also demonstrates that the performance of the RAKE receiver depends to a large extent on the underlying channel and hence the shape of the power delay profiles.

Acknowledgment

The authors would like to thank Dr. Fredrik Tufvesson at Lund University, Sweden, for useful comments and advice. The authors would also like to acknowledge Mr. Asim A. Ashraf in collaborating with the measurement campaign performed at MAX-Lab, Lund, Sweden.

References

[1] M.-G. di Benedetto, T. Kaiser and N. Schmidt *UWB – State of the Art*, Journal of Applied Signal Processing Editorial, EURASIP publishing, March 2005.

[2] U. S. Federal Communications Commission, FCC 02-48: First Report and Order.

[3] M. G. Khan, A. A. Ashraf, J. Karedal, F. Tufvesson, and A. F. Molisch, "Measurements and Analysis of UWB Channels in Industrial Environments," *in Proc. Wireless Personal Multimedia Communications (WPMC)*, Aalborg, Denmark, Sept. 2005.

[4] J. Karedal, S. Wyne, P. Almers, F. Tufvesson, and A. F. Molisch, "UWB channel measurements in an industrial environment", *in Proc. IEEE Globecom*, 2004.

[5] J. Karedal, S. Wyne, P. Almers, F. Tufvesson, and A. F. Molisch, "Statistical analysis of the UWB channel in an industrial environment," *in Proc. IEEE Vehicular Technology Conference*, 2004 fall.

[6] D. Cassioli, M. Z.Win, F. Vatalaro, and A. F. Molisch, "Performance of low-complexity Rake reception in a realistic UWB channel," *Proc. IEEE ICC'03*, vol.2, pp.763767, 2003.

[7] J. G. Proakis *Digital Communications*, 4th ed. Boston: McGraw-Hill, 2001.

[8] A. Rajeswaran, V.S. Somayazulu, J. R. Foerster, "RAKE performance for a pulse based UWB system in a realistic UWB indoor channel," *Proc. IEEE International Conference on Communications (ICC '03)* , vol.4, pp. 2879 - 2883, 11-15 May 2003.

[9] B. Mielczarek, M. Wessman, and A. Svensson, "Performance of coherent UWB RAKE receivers with channel estimators," *Proc. IEEE Vehicular Technology Conference*, vol. 3, pp. 1880-1884, Oct. 2003.

[10] G. Durisi, S. Benedetto, "Performance of coherent and noncoherent receivers for UWB communications ," *Proc. IEEE International Conference on Communications (ICC 2004)*, vol. 6, pp. 3429-3433, June 20-24, 2004.

[11] S. Gezici, H. Kobayashi, H. V. Poor and A. F. Molisch, "Optimal and suboptimal linear receivers for time-hopping impulse radio systems," *Proc. IEEE Wireless Communications and Networking Conference (WCNC 2004)*, vol. 2, pp. 908-913, Atlanta, GA, March 2004.

[12] E. Fishler and H. V. Poor, "On the tradeoff between two types of processing gain," *Proceedings of the 40th Annual Allerton Conference on Communication, Control and Computing*, Monticello, IL, Oct. 2-4, 2002.

[13] Y.-P. Nakache and A. F. Molisch, "Spectral shape of UWB signals influence of modulation format, multiple access scheme and pulse shape," *Proc. IEEE Vehicular Technology Conference, (VTC 2003-Spring)*, vol. 4, pp. 2510-2514, Jeju, Korea, April 2003.

[14] C.-C. Chong, Y. Kim and S. S. Lee, "A modified S-V clustering channel model for the UWB indoor residential environment," *Proc. IEEE Vehicular Technology Conference, (VTC 2005, Spring)*, p. in press, 2005.

[15] A. Saleh and R. Valenzuela, "A statistical model for indoor multipath propagation," *IEEE Journal on Select. Areas Commun.*, vol. SAC-5, no. 2, pp. 128-137, Feb. 1987.

[16] A. F. Molisch et al., "IEEE 802.15.4a channel model - final report," Tech. Rep. Document IEEE 802.15-04-0662-02-004a, 2005.

[17] A. F. Molisch et al., "An efficient low-cost time-hopping impulse radio for high data rate transmission," *Proc. IEEE 6th International Symposium on Wireless Personal Multimedia Communications (WPMC 2003)*, Yokosuka, Kanagawa, Japan, Oct. 19-22, 2003.

[18] S. Gezici, H. Kobayashi, H. V. Poor and A. F. Molisch, "Performance evaluation of impulse radio UWB systems with pulse-based polarity randomization in asynchronous multiuser environments," *Proc. IEEE Conference on Ultra Wideband Systems and Technologies (UWBST 2004)*, Kyoto, Japan, May 18-21, 2004.